Relationships between the Crystalline and the Smectic C Structures of a Biforked Mesogen

H. Allouchi* and M. Cotrait

Laboratoire de Cristallographie ERS 133 du CNRS, Université Bordeaux I, 351 cours de la Libération, F-33405 Talence Cedex, France

D. Guillon and B. Heinrich

Institut de Physique et Chimie des Matériaux de Strasbourg, Groupe des Matériaux Organiques, 20, rue du Loess, F-67037 Strasbourg Cedex, France

H. T. Nguyen

Centre de Recherche Paul Pascal, Domaine Universitaire, F-33405 Talence Cedex, France

Received January 24, 1995. Revised Manuscript Received September 14, 1995[⊗]

The crystal structure of a biforked mesogen containing thiobenzoate bis(4-[4-(3,4-dinonyloxy)benzoylthio]phenyl)-*trans*-1,4-cyclohexanedicarboxylate) is described. This compound exhibits interesting nematic and smectic phases. The molecule crystallizes in the $P\bar{1}$ space group ($Z = 2$) with one molecule per asymmetric unit, $a = 9.202(4)$ Å, $b = 10.139(2)$ Å, $c = 38.089$ Å, $\alpha = 96.05(1)°$, $\beta = 84.29(3)°$, and $\gamma = 96.71(3)°$. Molecules adopt a zigzag conformation, with the four alkoxy chains stretched and approximately parallel to the (*yoz*) plane; the mean axis of the alkoxy chains makes an angle close to 140° with the central core, and the molecules are arranged in sheets of about 38 Å thickness, as in a smectic C mesophase. The smectic C phase is analyzed by X-ray diffraction and dilatometry. The molecular arrangement in the mesophase is found to be very similar to that in the crystal phase, suggesting that the structure at room-temperature predetermines the type of mesophase observed at high temperature with small variations of the structural parameters.

1. Introduction

Polycatenar mesogens constitute a class of materials which molecules are formed by a long central aromatic core with several terminal aliphatic chains. Some phasmidic (three aliphatic end chains)[1] and biforked mesogens (two aliphatic end chains)[2,3] were synthesized and characterized through structural studies[4–7] in order to better understand the relation between the molecular structure and the mesomorphic behavior. In that respect, we began a systematic structural investigation of the crystalline phases for several biforked mesogens with thiobenzoate end groups and for several phasmidic compounds (six aliphatic substituents). Usually, phasmidic molecules exhibit columnar mesophases, whereas most of the biforked mesogens exhibit only smectic C phases. In this paper, we describe the three-dimensional crystallographic structure, at room temperature, of a new biforked mesogen with thiobenzoate end groups, and we compare it with the structural behavior (analyzed by X-ray diffraction and dilatometry) of the mesophase at high temperature.

The compound under study in the present paper has the following chemical formula:

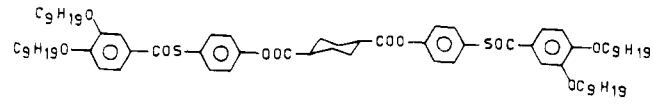

The synthesis and the first polymorphic characterization properties were published elsewhere.[7] Let us only recall, here its mesomorphic behavior as a function of temperature:

$$K \xrightarrow{124\ °C} S_C \xrightarrow{169\ °C} N \xrightarrow{180\ °C} I$$

2. Crystal Structure Analysis

2.1. Crystal Data and X-ray Measurements. Yellow plate crystals were obtained with some difficulties by slow evaporation from toluene solutions. They were brittle, soft and often twined. The crystal is flat with dimensions 0.25 × 0.075 × 0.025 mm. The unit-cell parameters were obtained by a least-squares fit of the setting angles of 25 reflections, with θ between 18 and 39°. The crystal data are given in Table 1 (see also Figure 1 for the atom labels).

The calculated density $d_c = 1.107$ g cm^{-3} is similar to that of other aliphatic and mesomorphic compounds

* Author to whom correspondence should be addressed.

[⊗] Abstract published in *Advance ACS Abstracts,* November 1, 1995.

(1) Malthête, J.; Levelut, A. M.; Nguyen, H. T. *J. Phys. Lett. (Paris)* **1985,** *46,* L875.
(2) Nguyen, H. T.; Destrade, C.; Levelut, A. M.; Malthête, J. *J. Phys. (Paris)* **1986,** *447,* 553.
(3) Destrade, C.; Nguyen, H. T.; Roubineau, A.; Levelut, A. M. *Mol. Cryst. Liq. Cryst.* **1988,** *159,* 163.
(4) Fang, Y.; Levelut, A. M.; Destrade, C. *Liq. Cryst.* **1990,** *7,* 267.
(5) Alstermark, G.; Eriksson, M.; Nilsson, M.; Destrade, C.; Nguyen, H. T. *Liq. Cryst.* **1990,** *8,* 75.
(6) Destrade, C.; Nguyen, H. T.; Alstermark, G.; Lindsten, G.; Nilsson, M.; Otterlholm, B. *Mol. Cryst. Liq. Cryst.* **1990,** *180B,* 265.
(7) Nguyen, H. T.; Destrade, C.; Allouchi, H.; Bideau, J. P.; Cotrait, M.; Guillon, D.; Weber, P.; Malthête, J. *Liq. Cryst.* **1993,** *15,* 4, 435.

0897-4756/95/2807-2252$09.00/0

Table 1. Crystal Data

$C_{70}H_{100}O_{10}S_2$	MW 1165.7 g mol^{-1}
triclinic	space group $P\bar{1}$ ($Z = 2$)
$a = 9.202(4)$ Å	$\alpha = 96.05(1)°$
$b = 10.139(2)$ Å	$\beta = 84.29(3)°$
$c = 38.089(5)$ Å	$\gamma = 96.71(3)°$
$v = 3496$ Å^3	R = 0.106 , wR = 0.115
$T = 298$ K	$d_{c=1.107}$ g.cm^{-3}
λ(Cu Kα) = 1.541 78 Å	μ(Cu Kα) = 1.09 mm^{-1}
crystal size 0.25 × 0.075 × 0.025 mm	no. of unique data ($I > 1.5\,\sigma(I)$) = 2123

containing long aliphatic chains.[8,9] The data were collected on a CAD-4 Enraf-Nonius diffractometer, equipped with a graphite monochromator, for the Cu Kα radiation (λ =1.5418 Å) with $(\sin\theta/\lambda)_{max} < 0.45$. Reflections between 2° and 45° ($0 \le h \le 8$, $-9 \le k \le 9$, $-34 \le l \le 34$) were collected with the $\omega-2\theta$ scan mode; scan range (3.0 + 0.15 tan θ)°, detector width (1.4 + 4.8 tan θ) mm. Three reflections (3 0 $\bar{12}$), ($\bar{3}$ 0 12) and (3 2 $\bar{11}$) were used as references and monitored every 200 reflections. The experimental absorption corrections were performed: the minimum and maximum transmission factors were 0.85 and 0.99 respectively. From 5558 measured reflections, only 2123 were considered as observed ($I > 1.5\sigma(I)$).

2.2. Structure Determination and Refinement. The crystal structure was solved by direct methods using the MITHRIL package.[10] The positions of all non-hydrogen atoms, except those for the extremities of all the alkyl chains which appeared after successive Fourier syntheses, are determined. The refinement by full matrix was performed using the SHELX76 package,[11] with anisotropic thermal factors for non-hydrogen atoms and by minimising $w(|F_o| - |F_c|)^2$ ($w = 1/\sigma(F_o)^2$). Hydrogen atoms were located in their theoretical position[12] and ride with the atoms to which they are attached.

As expected, polyaromatic central core atoms have a significantly smaller thermal motion than those of the alkyloxy chains. It has to be pointed out that the carbon atoms of the terminal alkyl chains present a very high thermal motion. Therefore, the refinement was resumed with constraint bond lengths[13] for the carbon-to-carbon distances of aliphatic chains, and with anisotropic temperature factors for non-hydrogen atoms. Scattering factors were used for non-hydrogen atoms[14] and for hydrogen atoms.[15] The final refinement converged to $R = 0.106$ with $wR = 0.115$; the residual electronic density is between −0.4 and 0.3 e Å^{-3}; $(\Delta/\sigma)_{max} = 0.3$. The rather limited number of observed reflections, according to the number of C, S, O atoms to be determined and the high thermal motion of alkoxy chains, may explain the relatively high R factor.

2.3. Molecular Structure. Atomic parameters (x/a, y/b, z/c, and U_{eq}) are given in Table 2. Bond lengths and bond angles are listed in Table 3. Surprisingly the asymmetric unit does not correspond to an entire molecule but to two half-molecules A and B, each of them adopts a different conformation. Moreover, the two different conformers in the cell are related by the symmetry centers (0, 0, $^1/_2$) and (0, $-^1/_2$, $^1/_2$). The molecular conformations of both moieties A and B are displayed with the SNOOPI program[16] along with the atomic labeling (Figure 1). Alkyl chains (C(32) to C(40)), (C(42) to C(50)), (C(82) to C(90)), and (C(92) to C(100)) are labeled (A,1), (A,2), (B,1), and (B,2) respectively.

The polyaromatic central cores C(1) to C(19) and C(51) to C(69) of half the molecules A and B and their homologues through the centers of symmetry have a significantly smaller motion than that reported for the alkyl chains as seen in Figure 2, especially for two of them: chain (A,1) and chain (B,1). For all chains the thermal atomic motion increased regularly from the attach point on the aromatic cycle toward the extremity of the chain. Chain (A,1) is very similar to chain (B,1); as chain (A,2) is very comparable to chain (B,2). The polyaromatic cores of molecules A and B have completely different conformations.

The cyclohexyl central rings φ_{0A} and φ_{0B} are defined by atoms C(1) to C(3) and C(51) to C(53) respectively together with their carbon atom homologues through the symmetry center, φ_{1A} and φ_{1B}, defined by atoms C(7) to C(12) and C(57) to C(62), respectively, the terminal cycles φ_{2A} and φ_{2B} defined by atoms C(16) to C(21) and C(66) to C(71), respectively, and both the (C−COO) and (C−COS) groups characterize the geometry of the polyaromatic central core.

The angles for C−COO and C−COS groups with the φ_0, φ_1, and φ_2 rings are different for molecule A or B. For molecule A, the angles are 57°, 65°, and 25.5°, respectively, for the C−COO group, whereas they are 42°, 47.7°, and 8.5°, respectively, for the C−COS group; the angle between the C−COS and C−COO groups being 18°. For molecule B, the angles are 34.3°, 65.5°, and 10.5°, respectively, for the C−COO group, whereas they are 29.7°, 60.8°, and 5.6°, respectively, for the C−COS group; the angle between the C−COS and C−COO groups being 4.9°.

The four benzene rings are perfectly planar. In molecule A, the angle between φ_1 and φ_2 is 39.4°. In molecule B, the angle between φ_1 and φ_2 is 55.6°. It is interesting to note that two terminal chains ((A,1), (B,1)) are in an extended zigzag planar conformation, whereas the second ones ((A,2), (B,2)) exhibit a gauche conformation initiated on the second carbon atom. The C−C−C−C torsion angles differ by less than 20° from 180°. This results in an almost parallel alignment of terminal chains. The significant torsion angles of the two independent half-molecules A and B are given in Table 4.

As far as the central aromatic part of the molecules is concerned, the torsion angles around C(1)−C(4) (C(2)−C(1)−C(4)−O(6)) for molecule A, and C(51)−C(54) (C(52)−C(51)−C(54)−O(56)) for molecule B are significantly different: 158° and 57°, respectively; in the crystal, the rotation is possible between the central

(8) Bideau, J. P.; Bravic, G.; Cotrait, M.; Nguyen, H. T.; Destrade, C. *Liq. Cryst.* **1991**, *10*, 3, 379.
(9) Merle, A.; Lamotte, M.; Risemberg, S.; Hauw, C.; Gaultier, J.; Grivet, J. P. *Chem. Phys.* **1977**, *22*, 207.
(10) Gilmore, C. J. Mithril: An Integrated Direct Methods Computer Program; *J. Appl. Crystallogr.* **1984**, *17*, 42.
(11) Sheldrick, G. M. *Shelx76, Program for Crystal Structure Determination*; University of Cambridge, England, 1976.
(12) Lehman, M. S.; Koetzle, T. F.; Hamilton, W. C. *J. Am. Chem. Soc.* **1972**, *94*, 2657.
(13) Gohring, S.; Fan, Z. X.; Haase, W.; Müller, M.; Gallardo, H. *Mol. Cryst. Liq. Cryst.* **1989**, *168*, 125.
(14) Cromer, D. T.; Waber, J. T. *International Tables for X-Ray Crystallography*; Ibers, V. A., Hamilton, W. C., Kynoch Press: Birmingham, 1974; Vol IV.
(15) Stewart, R. F.; Davidson, E. R.; Simpson, W. T. *J. Chem. Phys.* **1965**, *42*, 3175.
(16) Davies, K. SNOOPI, private communication, 1983.

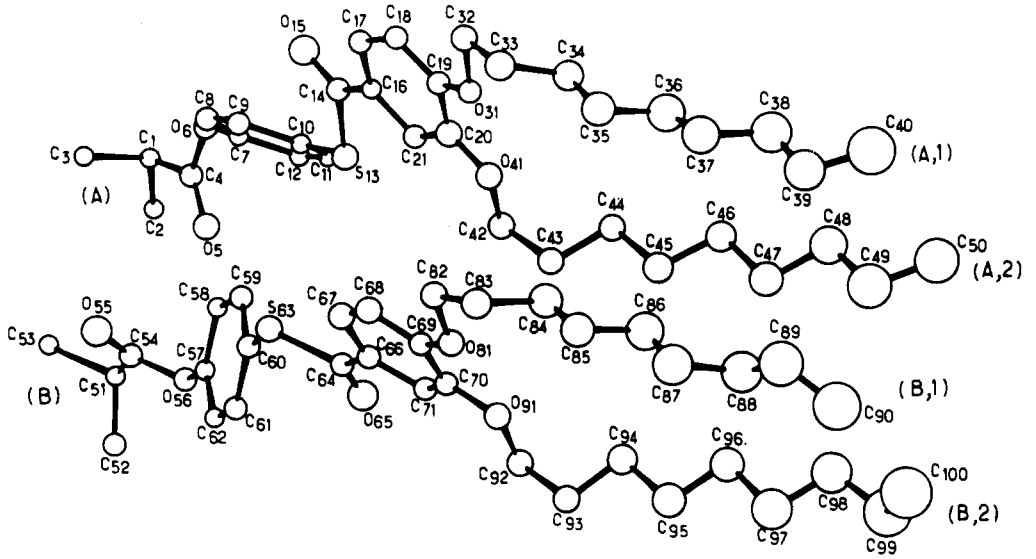

Figure 1. Molecular conformation and atomic labeling.

Table 2. Atomic Coordinates and Equivalent Thermal Parameters (Å²), $U_{eq} = {}^1/_3\Sigma_i\Sigma_j u_{ij} a_i^* a_j^* a_i a_j$

	x/a (10^4)	y/b (10^4)	z/c (10^4)	U_{eq} (10^3)		x/a (10^4)	y/b (10^4)	z/c (10^4)	U_{eq} (10^3)
C1	1091(12)	293(12)	4683(3)	44(8)	C51	1250(13)	−4428(14)	4789(4)	68(9)
C2	-136(11)	−775(11)	4642(3)	49(8)	C52	930(13)	−5899(11)	4760(3)	64(9)
C3	1573(11)	421(11)	5062(3)	47(8)	C53	879(12)	−3734(12)	5160(3)	65(9)
C4	2438(16)	−92(15)	4457(4)	67 (9)	C54	2908(19)	−4013(13)	4706(4)	81(9)
O5	2614(10)	−1198(9)	4332(3)	94 (8)	O55	3674(10)	−3446(10)	4915(2)	93(8)
O6	3352(10)	1016(8)	4391(2)	64(7)	O56	3366(9)	−4528(8)	4384(2)	66(7)
C7	4738(14)	873(12)	4196(4)	56(9)	C57	4900(13)	−4323(14)	4274(3)	55(9)
C8	5965(14)	1190(12)	4382(4)	67(9)	C58	5469(14)	−3006(13)	4229(3)	59(9)
C9	7295(14)	1077(11)	4187(4)	62(9)	C59	6930(14)	−2777(13)	4113(3)	62(9)
C10	7373(14)	600(11)	3824(3)	48(8)	C60	7758(14)	−3859(14)	4031(3)	56(9)
C11	6110(13)	327(12)	3655(3)	60(8)	C61	7160(15)	−5104(13)	4082(3)	70(9)
C12	4774(15)	365(12)	3848(4)	71(9)	C62	5673(15)	−5373(13)	4199(3)	66(9)
S13	9062(4)	313(4)	3580(1)	81(5)	S63	9716(4)	−3456(4)	3931(1)	84(5)
C14	10244(15)	1881(14)	3659(4)	73(9)	C64	9999(13)	−4256(12)	3494(3)	48(9)
O15	9929(10)	2707(10)	3876(3)	111(8)	O65	9076(10)	−4990(10)	3359(2)	103(8)
C16	11688(15)	1796(14)	3473(3)	57(9)	C66	11556(14)	−4108(13)	3355(4)	59(9)
C17	12797(14)	2828(13)	3538(4)	68(9)	C67	12620(16)	−3243(12)	3522(4)	81(9)
C18	14202(14)	2852(13)	3354(3)	67(9)	C68	14084(16)	−3083(13)	3376(4)	86(9)
C19	14483(16)	1853(15)	3085(4)	73(9)	C69	14450(16)	−3794(14)	3053(4)	68(9)
C20	13356(17)	778(15)	3017(4)	74(9)	C70	13378(18)	−4705(14)	2894(3)	73(9)
C21	12016(13)	810(13)	3189(3)	60(9)	C71	11942(14)	−4790(13)	3037(3)	65(9)
O31	15804(9)	1753(9)	2901(2)	82(8)	O81	15819(10)	−3796(10)	2877(2)	91(8)
C32	16973(13)	2811(12)	2956(3)	79(9)	C82	16894(14)	−2781(15)	3002(4)	111(9)
C33	18329(13)	2321(16)	2737(4)	144(9)	C83	18298(14)	−2872(15)	2757(4)	125(9)
C34	18096(16)	2020(15)	2346(4)	155(9)	C84	18076(15)	−2985(17)	2364(4)	170(9)
C35	19462(15)	1512((17)	2135(5)	176(9)	C85	19486(15)	−3272(19)	2135(5)	213(9)
C36	19156(18)	1105(22)	1748(5)	258(10)	C86	19197(19)	−3750(22)	1752(5)	317(10)
C37	20593(17)	802(21)	1527(5)	248(10)	C87	20671(18)	−4067(23)	1551(6)	332(10)
C38	20232(23)	564(24)	1139(6)	398(10)	C88	20369(21)	−4561(25)	1167(6)	573(10)
C39	21610(24)	44(24)	938(6)	410(10)	C89	21876(22)	−4531(24)	953(7)	400(10)
C40	21508(31)	11(33)	537(6)	872(10)	C90	21746(34)	−5555(25)	632(8)	883(10)
O41	13833(8)	−122(10)	2751(3)	84(8)	O91	13868(9)	−5459(10)	2592(3)	88(8)
C42	12776(14)	−1188(13)	2651(3)	81(9)	C92	12844(14)	−6433(14)	2426(3)	87(9)
C43	13549(14)	−2058(12)	2352(3)	84(9)	C93	13741(15)	−7249(13)	2141(4)	111(9)
C44	14029(16)	−1331(13)	2022(3)	110(9)	C94	14394(17)	−6412(14)	1844(4)	139(9)
C45	14826(16)	−2196(14)	1723(4)	130(9)	C95	15159(20)	−7342(15)	1553(4)	179(9)
C46	15304(19)	−1494(15)	1389(4)	167(9)	C96	15644(21)	−6632(16)	1220(4)	208(10)
C47	16004(20)	−2467(16)	1102(4)	189(9)	C97	16334(21)	−7544(18)	915(5)	234(10)
C48	16242(26)	−1785(19)	758(5)	293(10)	C98	16705(27)	−6822(22)	579(5)	380(10)
C49	16829(29)	−2804(20)	466(6)	400(10)	C99	17078(32)	−7860(23)	269(8)	677(10)
C50	17566(27)	−1942((22)	180(7)	459(10)	C100	18354(30)	−6943(26)	106(8)	677(10)

cyclohexane group and the rest of the molecule. The first torsion angle (158°) is very similar to that already found in another biforked mesogen structure.[7] It is interesting to note that the alkoxy chains adopt a completely trans conformation from atoms following the oxygen atom: for instance (A,1) is linear from C(32). As a result, both end chains can clearly be considered as rather flexible parts of the molecules, even in the crystalline phase.

The lengths of the four alkyl chains (A,1), (A,2), (B,1), and (B,2) (C(32) to C(40), C(42) to C(50), C(82) to C(90), and C(92) to C(100)) are quite similar: 10.0, 9.9, 9.6, and 9.5 Å, respectively. These chains are not strictly parallel. A small angle between the *main directions* of

Table 3. Bond Lengths (Å) and Angles (deg) with Standard Deviations

C1–C2	1.48(2)	C51–C52	1.48(2)	O5–C4 –O6	125.2(13)	O55–C54–O56	125.1(13)
C1 –C3	1.54(2)	C51–C53	1.54(2)	C4–O6–C7	118.9(10)	C54–O56–C57	117.9(10)
C1 –C4	1.50(2)	C51–C54	1.55(2)	O6–C7–C8	116.7(11)	O56–C57–C58	115.9(11)
C4 –O5	1.19(2)	C54–O55	1.17(2)	O6–C7–C12	119.0(11)	O56–C57–C62	119.7(11)
C4 –O6	1.35(2)	C54–O56	1.33(2)	C8–C7–C12	124.2(12)	C58–C57–C62	124.3(12)
O6 –C7	1.43(2)	O56–C57	1.43(2)	C7–C8–C9	115.8(12)	C57–C58–C59	117.5(12)
C7 –C8	1.38(2)	C57–C58	1.40(2)	C8–C9–C10	121.3(12)	C58–C59–C60	119.3(12)
C7 –C12	1.37(2)	C57–C62	1.34(2)	C9–C10–C11	119.8(11)	C59–C60–C61	120.7(12)
C8 –C9	1.38(2)	C58–C59	1.37(2)	C9–C10–S13	121.9(10)	C59–C60–S63	116.3(10)
C9 –C10	1.41(2)	C59–C60	1.40(2)	C11–C10–S13	118.4(9)	C61–C60–S63	122.1(10)
C10–C11	1.37(2)	C59–C61	1.34(2)	C10–C11–C12	119.5(12)	C60–C61–C62	121.4(12)
C10–S13	1.77(1)	C60–S63	1.81(1)	C7–C12–C11	118.6(12)	C57–C62–C61	116.7(12)
C11–C12	1.37(2)	C61–C62	1.40(2)	C10–S13–C14	104.4(6)	C60–S63–C64	101.8(6)
S13–C14	1.83(2)	S63–C64	1.78(2)	S13–C14–O15	122.3(11)	S63–C64–O65	122.6(10)
C14–O15	1.15(2)	C64–O65	1.18(2)	S13–C14–C16	110.7(10)	S63–C64–C66	112.2(9)
C14–C16	1.45(2)	C64–C66	1.47(2)	O15–C14–C16	125.7(13)	O65–C64–C66	124.1(12)
C16–C17	1.39(2)	C66–C67	1.39(2)	C14–C16–C17	119.0(12)	C64–C66–C67	122.8(12)
C16–C21	1.43(2)	C66–C71	1.37(2)	C14–C16–C21	124.2(12)	C64–C66–C71	117.9(12)
C17–C18	1.41(2)	C67–C68	1.40(2)	C17–C16–C21	116.2(12)	C67–C66–C71	119.1(12)
C18–C19	1.39(2)	C68–C69	1.39(2)	C16–C17–C18	122.4(12)	C66–C67–C68	121.5(13)
C19–C20	1.44(2)	C69–C70	1.41(2)	C17–C18–C19	119.3(12)	C67–C68–C69	118.3(13)
C19–O31	1.35(2)	C69–O81	1.37(2)	C18–C19–C20	118.9(13)	C68–C69–C70	119.6(13)
C20–C21	1.34(2)	C71–C71	1.38(2)	C18–C19–O31	124.2(13)	C68–C69–O81	126.5(13)
C20–O41	1.36(2)	C70–C91	1.38(2)	C20–C19–O31	116.6(12)	C70–C69–O81	113.7(12)
O31–C32	1.44(2)	O81–C82	1.42(2)	C19–C20–C21	120.0(13)	C69–C70–C71	120.3(13)
C32–C33	1.53(2)	C82–C83	1.52(2)	C19–C20–O41	110.9(12)	C69–C70–O91	115.8(12)
C33–C34	1.52(2)	C83–C84	1.52(2)	C21–C20–O41	128.9(13)	C71–C70–O91	123.9(13)
C34–C35	1.54(2)	C84–C85	1.53(2)	C16–C21–C20	122.7(12)	C66–C71–C70	120.9(12)
C35–C36	1.53(2)	C85–C86	1.53(3)	C19–O31–C32	119.1(10)	C69–O81–C82	115.6(11)
C36–C37	1.54(3)	C86–C87	1.54(3)	O31–C32–C33	105.4(10)	O81–C82–C83	108.1(11)
C37–C38	1.53(3)	C87–C88	1.54(3)	C32–C33–C34	112.3(12)	C82–C83–C84	114.4(12)
C38–C39	1.53(3)	C88–C89	1.54(3)	C33–C34–C35	111.2(12)	C83–C84–C85	111.5(12)
C39–C40	1.53(3)	C89–C90	1.52(4)	C34–C35–C36	110.3(14)	C84–C85–C86	112.0(14)
O41–C42	1.41(2)	O91–C92	1.43(2)	C35–C36–C37	109.7(15)	C85–C86–C87	107.7(16)
C42–C43	1.54(2)	C92–C93	1.53(2)	C36–C37–C38	106.5(16)	C86–C87–C88	107.4(17)
C43–C44	1.53(2)	C93–C94	1.52(2)	C37–C38–C39	104.6(17)	C87–C88–C89	106.2(18)
C44–C45	1.54(2)	C94–C95	1.55(2)	C38–C39–C40	109.8(20)	C88–C89–C90	108.0(20)
C45–C46	1.52(2)	C95–C96	1.53(2)	C20–O41–C42	115.3(10)	C70–O91–C92	118.4(10)
C46–C47	1.54(2)	C96–C97	1.54(3)	O41–C42–C43	106.1(10)	O91–C92–C93	106.3(10)
C47–C48	1.53(2)	C97–C98	1.53(3)	C42–C43–C44	112.9(10)	C92–C93–C94	111.2(11)
C48–C49	1.54(3)	C98–C99	1.54(4)	C43–C44–C45	113.0(11)	C93–C94–C95	107.6(12)
C49–C50	1.53(3)	C99–C100	1.53(4)	C44–C45–C46	114.0(12)	C94–C95–C96	111.1(13)
C2 –C1–C3	110.4(9)	C52–C51–C53	114.6(11)	C45–C46–C47	109.7(13)	C95–C96–C97	113.0(14)
C2 –C1–C4	110.2(10)	C52–C51–C54	110.8(11)	C46–C47–C48	107.3(14)	C96–C97–C98	111.2(16)
C3 –C1–C4	103.2(10)	C53–C51–C54	104.4(10)	C47–C48–C49	107.0(16)	C97–C98–C99	108.2(19)
C1 –C4–O5	124.8(13)	C51–C54–O55	124.0(13)	C48–C49–C50	103.6(18)	C98–C99–C100	93.7(20)
C1 –C4–O6	109.7(11)	C51–C54–O56	110.5(12)				

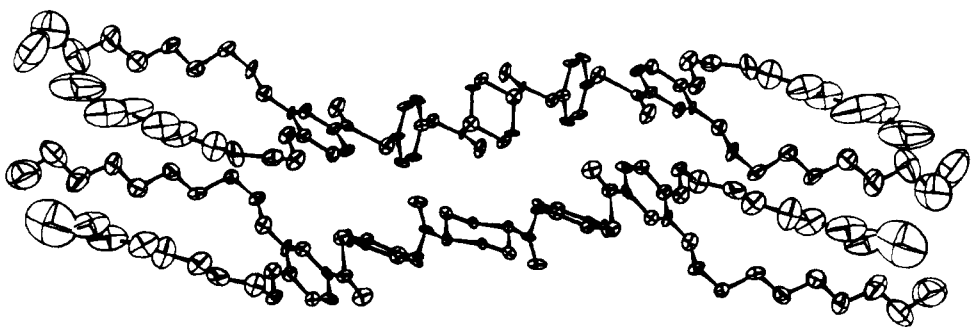

Figure 2. Snoopy drawing of the molecules.

Table 4. Significative Torsion Angles (deg) with Standard Deviations

C(3)–C(1)–C(4)–O(6)	−84(1)	C(59)–C(60)–S(63)–C(64)	−121(1)
C(2)–C(1)–C(4)–O(6)	158(1)	S(63)–C(64)–C(66)–C(67)	−11(1)
C(4)–O(6)–C(7)–C(8)	−110(1)	C(68)–C(69)–O(81)–C(82)	−14(1)
C(9)–C(10)–S(13)–C(14)	−52(1)	O(31)–C(32)–C(33)–C(34)	59(1)
C(10)–S(13)–C(14)–O(15)	12(1)	O(41)–C(42)–C(43)–C(44)	−63(1)
C(52)–C(51)–C(54)–O(56)	57(1)	O(81)–C(82)–C(83)–C(84)	48(1)
C(54)–O(56)–C(57)–C(58)	−66(1)	O(91)–C(92)–C(93)–C(94)	−68(1)

two terminal chains exists, namely 12.1° between (A,1) and (A,2), and 13.7° between (B,1) and (B,2); however, both chains are parallel to the ($y0z$) plane. The length of the central core of molecules A and B is identical (29.1 Å). The mean planes of chains (A,1) and (A,2) make an angle of 65° between each other; the mean planes of chain (B,1) and (B,2) molecule make an angle close to 80° between each other. As mentioned above, the thermal motion for (A,1) and (B,1) alkoxy chains is much higher than that of (A,2) and (B,2) (Figure 2).

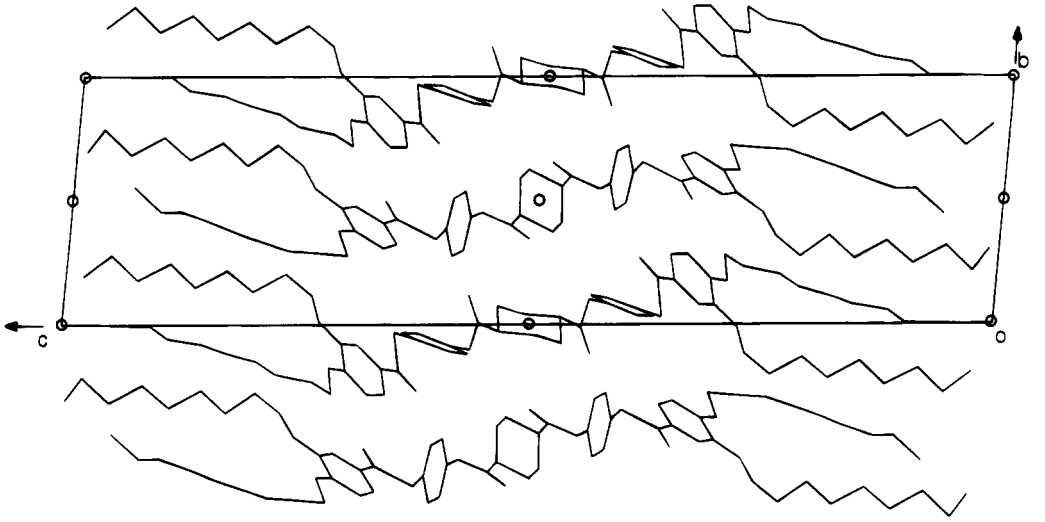

Figure 3. Projection of the structure along the *a* axis.

2.4. Molecular Packing and Arrangement. The projection of the structure along the *a* axis is shown in Figure 3. The cohesion of the crystal is almost entirely due to van der Waals forces between the polyaromatic central cores related by symmetry centers, located at $x = 0.5$. Only very few interactions involve alkyloxy chains between neighboring molecules. The molecules give two-dimensional sheets, parallel to the plane (*xoy*), whose thickness is about 38 Å, corresponding to the length of the *c* parameter. The interactions between sheets involving the terminal methyl groups at $z = 0.0$ and $z = 1.0$ are very weak. The molecular arrangement is typical of a lamellar structure with segregation of the aliphatic chains and central polyaromatic cores into three distinct sublayers. It is then possible to define molecular layers as they are in the smectic C phase. Both aliphatic chains are approximately perpendicular to the layer plane. The polyaromatic cores are aligned, quasi-parallel, and are tilted with an angle of 55° with respect to the layer plane. The projection of the molecular packing on the (*xoz*) plane is illustrated in Figure 4, where the zigzag shape of the molecules is obvious.

Let us note that, in a structure reported previously[8] on another biforked mesogen, the angle between the two main directions of the terminal chains was found to be about 40°; in that case, a columnar mesophase was observed. For the compound under consideration, the same angle is much smaller, about 12°, and only a smectic C phase is observed. A more detailed analysis of the relationships between the crystallographic structure of the solid phase at room temperature and the type of mesophase observed at high temperature will be published in a forthcoming paper for a large number of biforked compounds.

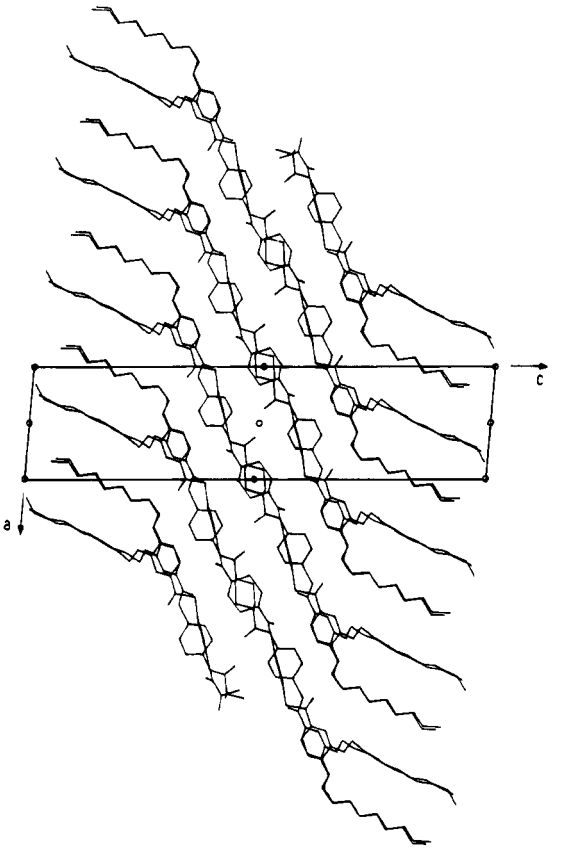

Figure 4. Projection of the structure along the *b* axis.

3. Structural Study of the Mesophase

3.1. X-ray Diffraction. X-ray diffraction experiments were performed as a function of temperature using a Guinier focusing camera,[17] equipped with a bent quartz monochromator (Cu $K\alpha_1$ radiation) and a heating sample holder operating under vacuum. The powder patterns of the liquid-crystal compound in Lindemann capillaries were recorded photographically or using a curved position-sensitive detector. A typical pattern of the smectic C phase of this compound is shown in Figure 5. It consists, as usual for mesogen compounds, of one sharp Bragg reflections in the small-angle region and a diffuse band in the wide angle region. The layer spacing in the smectic C phase is found to be 33.5 Å at 150 °C and should be compared with the overall molecular length, 52.4 Å, as determined from molecular simulations. At a first approximation these values indicate that the molecular tilt in the smectic C phase is about 50° with respect to the layer normal.

It is interesting to note that the layer spacing is smaller than the crystalline phase (38 Å). In the same time, the average tilt angle of the molecules, estimated

(17) Guinier, A. *Théorie et technique de radiocristallographie*; Dunod: Paris, 1964.

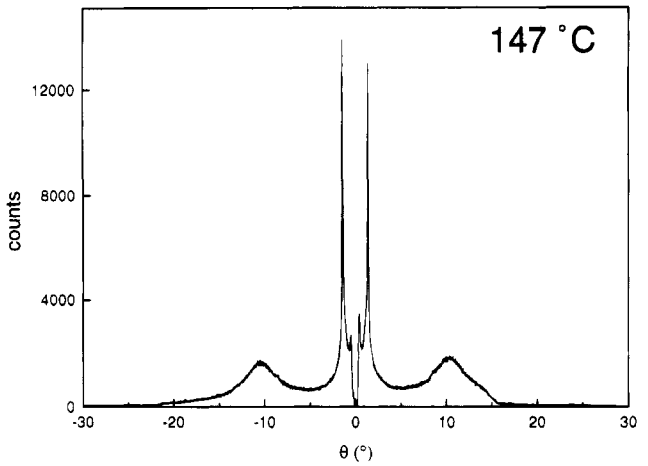

Figure 5. Typical example of X-ray diffraction pattern registered in the smectic C phase.

from the layer spacing and the molecular length is 50°, similar to that determined in the crystalline phase for the only rigid aromatic cores of the molecules. As a consequence, one can suppose that when melting during the crystal-to-smectic transition, the average direction of the disorganized aliphatic chains becomes closer to that of the aromatic cores or that the molten aliphatic chains spread laterally at the interfaces between smectic layers and contribute to a decrease of the layer spacing.

3.2. Volumetric Study. High-resolution volumetric measurements were performed in order to obtain the value of the molecular area S in the mesomorphic smectic C phase. The volumetric data were measured with a dilatometer of the Bekkedahl type[18] using a new setup described elsewhere.[19] The dilatometer was filled with about 1 g of the sample and immersed in a large oil bath, which temperature was regulated to within 0.05 K. The sample inside the dilatometer was degassed and capped with mercury. With this setup, the various transition temperatures were stable over a very long period (several days) covering warming and cooling runs. The variations of the specific volume were determined from the changes in the height of the mercury column. The mercury level was read thanks to a thin laser beam and stored together with temperature on a computer. Changes in specific volume as small as $\sim 10^{-4}$ cm^3/g were regularly resolved. The measurements were made at equilibrium, with each temperature being kept constant for a period of 1 mn, before to be changed with a step of 0.1 K (heating run) or −0.1 K (cooling run).

Figure 6 shows the variation of the specific volume versus temperature (heating) from the crystalline phase up to the isotropic phase. The transition from the crystalline to the smectic C phase is clearly of first order and characterized by a large volume jump in a narrow temperature range, namely, $\Delta v/v \cong 8.6\%$ ($\Delta v = 136.8$ Å^3 for one molecule). The two other transitions (smectic C → nematic and nematic → isotropic, see Figures 7 and 8) are also of first order, but the corresponding volume jumps are much smaller ($\Delta v/v = 0.3\%$ with $\Delta v = 6$ Å^3 at Sc → N and 0.5% with $\Delta v = 8.8$ Å^3 at N → I transition). It is important to note that these transitions are characterized by pretransitional effects where the specific volume does not vary any more linearly with the temperature; nevertheless, the phases are characterized by large temperature domains where the volume is a linear function of temperature, with thermal expansion coefficients of $\alpha = 1/V(\partial V/\partial T) = 4.1$, 7.5, 9.7, and 9.5×10^{-4} K^{-1} for the crystalline, smectic C, nematic and isotropic phases, respectively. These values are in

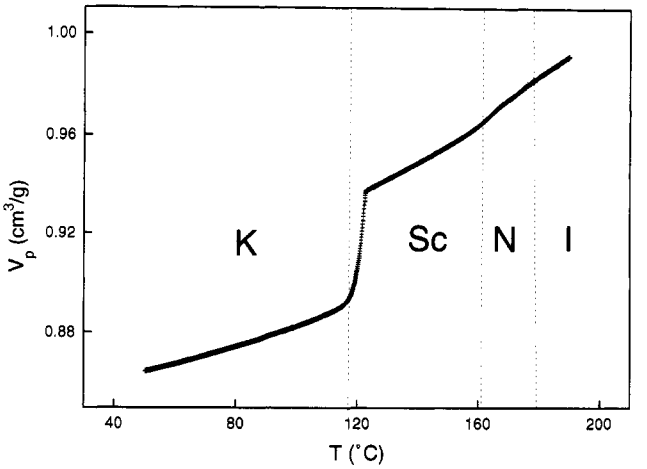

Figure 6. Specific volume as a function of temperature obtained with heating run. Vertical dashed lines are phase boundaries.

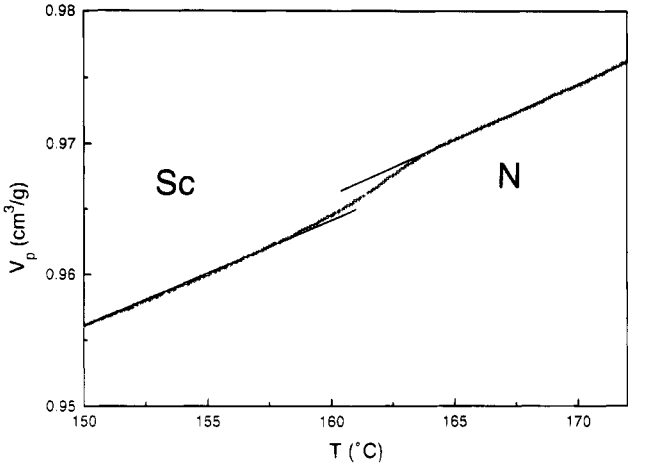

Figure 7. Specific volume in the smectic C and nematic phases. Lines represent the linear fit of V_p as a function of T within the stability domain of each phase.

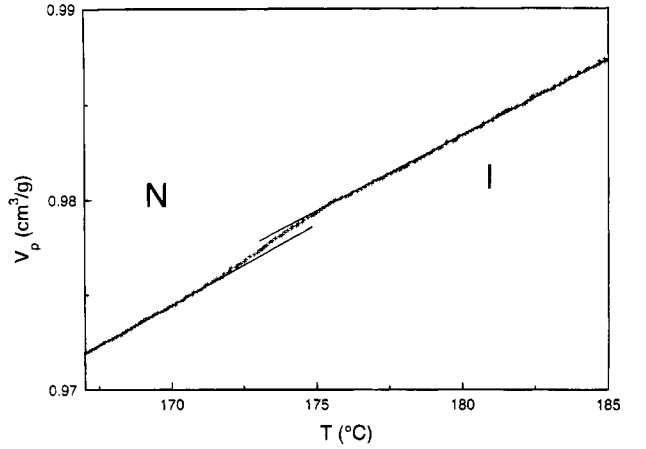

Figure 8. Specific volume in the nematic and isotropic phases. Lines represent the linear fit of V_p as a function of T within the stability domain of each phase.

(18) Bekkedahl, N. *J. Res. Natl. Bur. Stand.* **1949**, *42*, 145.
(19) Heinrich, B.; Halbwachs, A.; Skoulios, A.; Guillon, D., to be published.

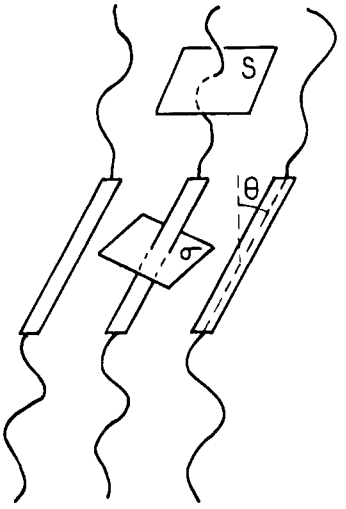

Figure 9. Molecular area (S) and lateral bulkiness (σ) of the molecules in the smectic C phase.

good agreement with previous ones already reported for the same type of phases with other liquid crystal compounds.[20] Finally, let us point out that these specific volume values were perfectly reproductible in the smectic, nematic, and isotropic phases, whenever they were obtained through heating or cooling runs.

For a lamellar system such as a smectic C mesophase, particularly when the molecules are symmetrical with identical aliphatic chains at their extremities, the molecular area S has a very simple geometrical sense. It represents the average surface per molecule in the plane of the smectic layers.[21] Clearly, the molecular area is directly related to the molar volume V and to the layer spacing d by $S = V/Nd$, where N is Avogadro's number. It should be emphasized that S must not be confused with σ, which is the average area per molecule in a plane perpendicular to the long axis of the molecule[21] (Figure 9). The latter offers a specific measure of the compactness in the lateral packing of the molecular arrangement. Of course, when the molecules are tilted at an angle θ with respect to the layer normal, σ is given by $\sigma = S \cos(\theta)$.

From the experimental values of the molar volume and of the smectic C layer spacing, the molecular area S of the compound under study was found to be about 54.9 Å^2. As a consequence, each aliphatic end chain occupies an area of 27.5 Å^2. This situation is in very good agreement with that determined, for example, in the case of the smectic C phase of TBDA.[22] From the crystallographic study reported above, it is possible to calculate the area σ of each aromatic core, which is equal to 26 Å^2 at 25 °C and which can be estimated to 27 Å^2 at 150 °C[22] by taking into account the lateral thermal expansion. Thus, the tilt angle of the aromatic cores within the smectic C layers can be estimated to about 60°, at 150 °C, similar to the value determined in the crystalline phase. The aromatic sublayer is then deduced from the length of the aromatic core (l_A = 29.1 Å; see section 2.3) through the relation $d_A = l_A \cos 60 \approx$ 14.5 Å, and consequently the thickness of each aliphatic sublayer can be estimated to be about 9.5 Å in the smectic C phase; this value corresponds roughly to the average aliphatic chain length (9.7 Å). Thus it is easy to conclude that the aliphatic chains are also oriented almost normal to the smectic layers, simularly as in the crystalline phase.

Therefore, from the crystal to the smectic C mesophase, the average tilting directions of the aromatic cores and of the aliphatic end chain of the molecules do not significantly vary. As a matter of fact, we can conclude that the overall crystallographic molecular arrangement at room temperature seems to predetermine the molecular arrangement in the mesophase at high temperature, with only very small variations of the structural parameters.

Supporting Information Available: Observed and calculated structure factors (14 pages). Ordering information is given on any current masthead page.

CM950040F

(20) Seurin, P.; Guillon, D.; Skoulios, A. *Mol. Cryst. Liq. Cryst.* **1981**, *65*, 85. Poeti, G.; Fanelli, E.; Torquati, G.; Guillon, D. *Il Nuovo Cimento* **1983**, *1*, 1335.

(21) Guillon, D.; Skoulios, A. *Mol. Cryst. Liq. Cryst.* **1977**, *38*, 31.

(22) Guillon, D.; Skoulios, A., Benattar, J. J. *J. Phys.* **1986**, *47*, 133.